DØ Note 5715-CONF

A search for charged Higgs bosons in $t\bar{t}$ events.

The DØ Collaboration

(Dated: July 28, 2008)

We present a search for charged Higgs bosons in top quark decays with masses below the top quark mass. We use the e+jets, μ+jets, ee, $e\mu$, $\mu\mu$, $\mu+\tau$ and $e+\tau$ channels of the $t\bar{t}$ final state with approximately 1 fb^{-1} of integrated luminosity. We consider a model with pure tauonic decays of the charged Higgs which would manifest itself as a deficit of the expected number of events compared to the standard model (SM) prediction in all but the τ+lepton channel. We also study a leptophobic model where a pure hadronic decay of a charged Higgs boson is assumed. This would lead to a suppression of the expected number of $t\bar{t}$ events in all channels considered. We extract limits on the $\mathcal{B}r(t \to H^+b)$ for tauonic and leptophobic charged Higgs models. For the latter we exclude $\mathcal{B}r(t \to H^+b) > 0.2$ for the charged Higgs masses between 80 and 155 GeV. For the tauonic model the excluded branching fractions range from 0.12 at low Higgs boson mass up to 0.2 at high mass. For the SM case ($\mathcal{B}r(t \to H^+b) = 0$) we perform a combination of the top quark pair production cross sections measurements in different final states.

Preliminary Results for Summer 2008 Conferences

I. INTRODUCTION

The top quark pair production cross section $\sigma_{t\bar{t}}$ and $\mathcal{B}r(t \to W^+b)$ are known to high accuracy in the standard model (SM). Exotic non-W decays of the top quark could lead to deviations from the SM $\sigma_{t\bar{t}} \cdot \mathcal{B}r$ for individual decay channels of $t\bar{t}$ events.

Many extensions of the SM, including Supersymmetry and Grand Unified Theories, require the existence of an additional Higgs doublet. Such models predict additional physical Higgs particles, including three neutral and two charged Higgs bosons ($H^{\pm}$). If a charged Higgs boson is sufficiently light it can appear in top quark decays $t \to H^+b$. A non-vanishing branching fraction to a charged Higgs boson would lead to a decrease of branching fraction to a W boson expected in the SM top quark decays.

Based on the top quark pair production cross sections measured in various $t\bar{t}$ decay modes, we search for the presence of charged Higgs bosons in top quark decays. Within the SM, the top quark decays into a W boson and b quark nearly 100% of the time, and the $t\bar{t}$ event signature is fully determined by the W boson decay modes. In the presence of a charged Higgs boson the $t \to H^+b$ decay will compete with the SM top quark decay $t \to W^+b$. The branching fractions of a charged Higgs boson depend on the ratio of the vacuum expectation values of the two Higgs doublets, $\tan\beta$. For small values of $\tan\beta$ it is dominated by the decay to charm and strange quarks. For larger values of $\tan\beta$ it is dominated by the decay to a τ lepton and a τ neutrino (see Fig. 1). Thus, given a certain $t\bar{t}$ production cross section, the presence of a charged Higgs boson significantly modifies the expected number of events in different final states of a top quark pair.

We consider two models for the charged Higgs boson decay: a purely tauonic model, where the charged Higgs decays exclusively into a τ lepton and neutrino, and a purely leptophobic model, where the charged Higgs boson decays into a charm and a strange quark. The tauonic model is identical to the minimal supersymmetric standard model (MSSM) for large values of $\tan\beta$. A scenario in which the charged Higgs boson decays into quarks with a 100% branching fraction can be realised, for instance, in a general multi-Higgs-doublet model (MHDM) [3]. It was demonstrated that such leptophobic charged Higgs boson with a mass of about 80 GeV could lead to noticeable effects at the Tevatron if $\tan\beta \leq 3.5$ [4]. Moreover, large radiative corrections from SUSY-breaking effects can lead to a suppression of $H^+ \to \tau^+\nu$ compared to $H^+ \to c\bar{s}$ [5, 6]. In that case, for small $\tan\beta$, both 2HDM models [4] and the MSSM can become similar to the leptophobic model.

In this analysis we consider the following final states of a top quark pair: the dilepton channel where both charged bosons ($W^{\pm}$ or $H^{\pm}$) decay into a light charged lepton (e or μ) either directly or through the leptonic decay of a τ, the τ+lepton channel where one charged boson decays to a light charged lepton and the other one to a τ-lepton decaying hadronically, and the lepton plus jets (ℓ+jets) channel where one charged boson decays to a light charged lepton and the other decays into hadrons. For the tauonic charged Higgs model an increased number of events is expected in the τ+lepton channel compared to the SM, while in all other considered channels the number of events should decrease. The presence of a leptophobic charged Higgs boson would lead to migration of events from the dilepton and ℓ+jets channels to the all-hadronic channel. As a result, we expect to see a deficiency of events in all considered channels.

For the tauonic charged Higgs model we consider two possibilities. In the first case we fix the $t\bar{t}$ cross section to the theoretical SM next-to-leading order calculaltion and extract the $Br(t \to H^+b)$. In the second case, we fit $\sigma_{t\bar{t}}$ and $Br(t \to H^+b)$ simultaneously, thus extracting a limit free of the assumption about the $t\bar{t}$ cross section. The simultaneous fit requires a reasonably small correlation between the two observables. Therefore it is not possible to perform it if only disappearance channels are present in the fit as in the case of leptophobic model.

The analysis is based on data collected with the DØ detector between August 2002 and April 2006 at the Fermilab Tevatron $p\bar{p}$ collider at $\sqrt{s} = 1.96$ TeV. The analyzed datasets correspond to an integrated luminosity of about 1 fb^{-1}.

CDF reported a search for charged Higgs bosons using different decay modes with a data set of about 200 pb^{-1} [7]. They excluded $Br(t \to H^+b) > 0.4$ for tauonic decaying charged Higgs bosons at 95% C.L. A recent search for leptophobic decaying charged Higgs bosons by CDF [8] using a template method, results in the exclusion of $Br(t \to H^+b) > 0.1$ to $Br(t \to H^+b) > 0.3$ dependent on the charged Higgs mass.

II. DØ DETECTOR

The DØ detector includes a tracking system, calorimeters, and a muon spectrometer [9]. The tracking system consists of a silicon microstrip tracker (SMT) and a central fiber tracker (CFT), both located inside a 2 T superconducting solenoid. The tracker design provides efficient charged particle measurements in the pseudorapidity [10] region $|\eta| < 3$. The SMT strip pitch of 50–80 μm allows a precise reconstruction of the primary interaction vertex (PV) and an accurate determination of the impact parameter of a track relative to the PV [11], which are the key components of the lifetime-based b-jet tagging algorithms. The calorimeter consists of a central section (CC) covering $|\eta| < 1.1$, and two end calorimeters (EC) extending the coverage to $|\eta| \approx 4.2$. The muon system surrounds the

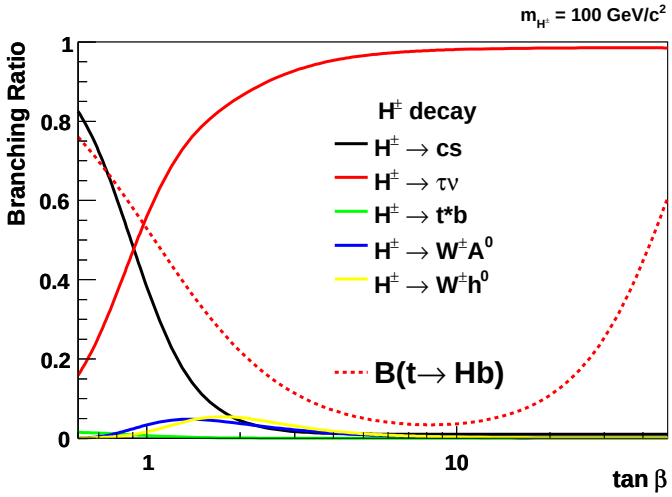

FIG. 1: The branching ratio for top decays assuming that $\mathcal{B}r(t \to W^+b) + \mathcal{B}r(t \to H^+b) = 1$ and the branching ratio for charged Higgs decays for $M_{H^\pm} = 100$ GeV. Calculation is performed using CPsuperH [1] with a set of MSSM parameters corresponding to benchmark 4 of [2]. CPsuperH includes QCD and supersymmetric QCD and electroweak radiative corrections up to the two-loop leading logarithms. These corrections are applied to the top and bottom quark Yukawa couplings.

calorimeter and consists of three layers of tracking detectors and two layers of scintillators [12]. A 1.8 T iron toroidal magnet is located outside the innermost layer of the muon detector. The luminosity is calculated from the rate for $p\bar{p}$ inelastic collisions detected using two hodoscopes of scintillation counters mounted close to the beam pipe on the front surfaces of the EC calorimeters.

III. EVENT SELECTION

In this analysis we search for the charged Higgs boson using ℓ+jets, dilepton and $\ell + \tau$ final states of a $t\bar{t}$ pair. All channels are constructed to be orthogonal in order to do a simple maximum likelihood fit to the observables. Orthogonality between the dilepton channels is achieved by vetoing events that contain an isolated electron in the $\mu\mu$ and a second electron in the $e\mu$ channel. We veto a muon and a second electron in the e+jets channel and reject events that pass the $\ell + \tau$ selection. In the μ+jets channel we reject events that pass the $\mu\mu$ or $\ell + \tau$ selections or contain an isolated electron. Orthogonality between the $e + \tau$ channel and the dilepton channels is achieved by rejecting events with a muon or a second electron in the $e + \tau$ selection. In the $\mu + \tau$ channel, similar to the μ+jets channel, we reject events that pass the $\mu\mu$ selection or contain an electron.

In the ℓ+jets channel we select a data sample enriched in $t\bar{t}$ events by requiring ≥ 3 jets with transverse momentum $p_T > 20$ GeV and pseudorapidity $|\eta| < 2.5$, one isolated electron (muon) with $p_T > 20$ GeV and $|\eta| < 1.1$ ($|\eta| < 2.0$), and missing transverse energy $\not\!\!E_T > 20$ GeV (e+jets) or $\not\!\!E_T > 25$ GeV (μ+jets). The leading jet p_T is required to exceed 40 GeV.

To select the dilepton and $\ell + \tau$ events we require one isolated lepton (e or μ) for the $\ell + \tau$ channel or two isolated oppositely charged leptons for the ee, $\mu\mu$ and $e\mu$ channels. The τ candidates are required to have a high output value of the dedicated identification neural network. We accept events with at least two jets within $|\eta| < 2.5$, one of which has to have $p_T > 30$ GeV and the other $p_T > 20$ GeV. In $e\mu$ channel, we also accept events with one jet. In the $l + \tau$ channels, a jet matched within $\Delta R < 0.5$ to the selected tau candidate is removed. Leptons are required to have $p_T > 15$ GeV in the ee, $\mu\mu$ and $e\mu$ channels while an electron (muon) with $p_T > 20$ GeV is required in the $e\tau$ ($\mu\tau$) channels. Muons are accepted in the region $|\eta| < 2.0$. Electrons must be within $|\eta| < 1.1$ in $e\tau$ channel and within $|\eta| < 1.1$ or $1.5 < |\eta| < 2.5$ in ee and $e\mu$ channels.

To improve the signal over background ratio in the ℓ+jets and the $\ell + \tau$ channels at least one identified b-jet is required while in the dilepton channels topological cuts are applied.

More details on the event selection in the different channels and the composition of the relevant background can be found in Refs. [13–15].

The expected and observed numbers of events in various search channels are summarized in Table I. The yields are shown for the SM case of $\mathcal{B}r(t \to H^+b) = 0$. The $t\bar{t}$ contribution is calculated for a theoretical $t\bar{t}$ cross section of

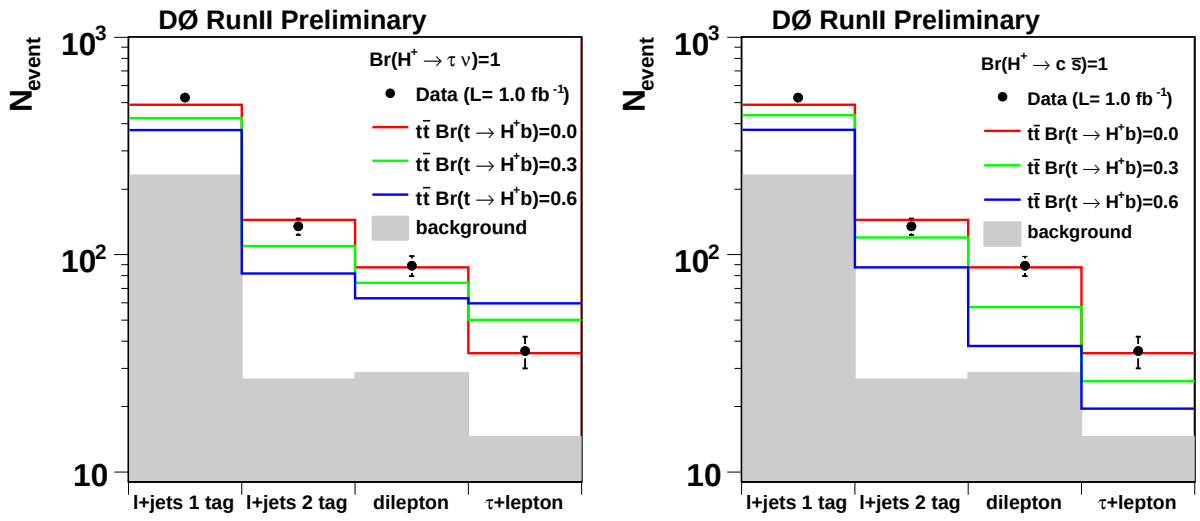

FIG. 2: Predicted and observed number of events for different $\mathcal{B}r(t \to H^+b)$ in the tauonic (left) and leptophobic (right) model.

$\sigma_{t\bar{t}} = 7.91$ pb [16, 17] for a top quark mass of 170 GeV. Since the limits on the charged Higgs production are sensitive to the choice of the theoretical cross section and its uncertainty, for the charged Higgs search we assume the world average top quark mass [18]. Figure 2 shows the observed number of events in different analysis channels compared to the prediction for different values of $\mathcal{B}r(t \to H^+b)$ for tauonic (left plot) and leptophobic (right plot) models.

Channel	$t\bar{t}$	$t\bar{t}$+background	observed
e+jets 3 jets 1tag	79.04 ± 0.32	180.73 ± 4.71	183
e+jets $\geq$ 4 jets 1tag	78.94 ± 0.31	100.95 ± 2.23	113
e+jets 3 jets 2tag	29.71 ± 0.15	40.40 ± 1.16	40
e+jets $\geq$ 4 jets 2tag	40.35 ± 0.18	43.59 ± 0.89	30
μ+jets 3 jets 1tag	57.03 ± 0.27	140.81 ± 3.78	133
μ+jets $\geq$ 4 jets 1tag	63.69 ± 0.27	82.11 ± 2.34	99
μ+jets 3 jets 2tag	23.05 ± 0.13	32.61 ± 1.19	31
μ+jets $\geq$ 4 jets 2tag	34.44 ± 0.16	36.99 ± 1.00	34
ee	11.22 ± 0.14	14.59 ± 0.4	17
$e\mu$ 1jet	8.58 ± 0.11	18.08 ± 0.66	21
$e\mu$ 2jets	35.19 ± 0.17	44.55 ± 0.69	39
$\mu\mu$	8.79 ± 0.10	15.15 ± 0.57	12
$e + \tau$	10.31 ± 0.18	14.66 ± 1.75	16
$\mu + \tau$	12.15 ± 0.17	22.31 ± 2.85	20

TABLE I: Expected and observed yields in the various channels for the SM top quark decays and $\sigma_{t\bar{t}} = 7.91$ pb. The uncertainties are statistical only.

IV. STANDARD MODEL CROSS SECTION COMBINATION

To estimate cross section σ_j in an individual channel j the following likelihood function is defined:

$$\mathrm{L}(\sigma_j, \{N_j^{\mathrm{obs}}, N_j^{\mathrm{bkg}}, \mathcal{B}r_j, \mathcal{L}_j, \varepsilon_j\}) \;=\; \mathcal{P}(N_j^{\mathrm{obs}}, \mu_j) = \frac{\mu_j^{N_j^{\mathrm{obs}}}}{N_j^{\mathrm{obs}}!}\, e^{-\mu_j}, \tag{1}$$

where $\mathcal{P}(N_j^{obs}, \mu_j)$ is the Poisson probability of expected μ_j signal-plus-background events:

$$\mu_j \;=\; \sigma_j\, \mathcal{B}r_j\, \mathcal{L}_j\, \varepsilon_j + N_j^{bkg} \tag{2}$$

to be compatible with the number of observed events N_j^{obs} given the luminosity $\mathcal{L}_j$, branching fraction $\mathcal{B}r_j$, signal efficiency ϵ_j and expected number of background events N_j^{bkg}.

For the combination of all channels, we construct a binned likelihood function consisting of 14 bins corresponding to the following channels: ℓ+jets with electron or muon, 3 or ≥ 4 jets and 1 or ≥ 2 b-tags, dilepton with ee, $\mu\mu$ and $e\mu$ with ≥ 2 jets $e\mu$ with 1 jet, and $\ell + \tau$ with electron or muon, at least one b-tag and ≥ 2 jets. We include the systematic uncertainties as nuisance parameters [19] into the fit. Each source of systematics is represented by a Gaussian term centered at zero and with a standard deviation of one. It is allowed to float during the maximization procedure. The correlations are taken into account in a natural way, by letting the same nuisance parameter affect different variables. The total likelihood function that is maximized is the product of L and L_s, with

$$\mathrm{L}_s = \prod_i \mathcal{G}(\nu_i; 0, 1)\,,$$

where $\mathcal{G}(\nu_i; 0, 1)$ is the normal probability of the nuisance parameter i to take the value ν_i.

Using this method we extract the SM top quark pair production cross section for the combined ℓ+jets, dilepton and τ+lepton channels. The SM cross section at the top quark mass of 170 GeV yields

$$\sigma_{\bar{t}} \;=\; 8.16^{+0.80}_{-0.72}(\mathrm{stat{+}syst}) \pm 0.50(\mathrm{lumi})\ \mathrm{pb}\ .$$

For a top quark mass of 175 GeV, the combined $t\bar{t}$ cross section is fitted as

$$\sigma_{\bar{t}} \;=\; 7.83^{+0.77}_{-0.70}(\mathrm{stat{+}syst}) \pm 0.48(\mathrm{lumi})\ \mathrm{pb}\ .$$

Table II shows the separate result for the ℓ+jets and dilepton channel at a top quark mass of 175 GeV. As shown in Fig. 3 the combined cross section depends on the top quark mass and can be parameterized as $\sigma_{t\bar{t}} = (44.27 - 0.19 \cdot m_{top}/\mathrm{GeV} - 0.001 \cdot m_{top}^2/\mathrm{GeV}^2 + 0.000006 \cdot m_{top}^3/\mathrm{GeV}^3)$ pb.

channel	$\sigma_{t\bar{t}}$ [pb]
ℓ+jets	$8.20^{+0.52}_{-0.50}$ (stat)$^{+0.77}_{-0.66}$ (syst) $\pm$ 0.50 (lumi)
dilepton	$7.03^{+1.12}_{-1.04}$ (stat)$^{+0.78}_{-0.59}$ (syst) $\pm$ 0.43 (lumi)

TABLE II: $\sigma_{t\bar{t}}$ in the individual channels, fitted with the nuisance parameter method. The results are given at a top quark mass of 175 GeV.

Table III shows the breakdown of the systematic uncertainties on $\sigma_{t\bar{t}}$. The main sources of systematic uncertainties include b-tagging [20], event preselection, lepton identification and jet energy calibration. The uncertainty on event preselection comes from primary vertex selection and data quality requirements which are fully correlated among ℓ+jets, dilepton and τ+lepton channels.

V. EVENT EXPECTATION IN DIFFERENT SIGNAL CHANNELS

We use Monte Carlo (MC) simulations to calculate the number of expected events from the charged Higgs decays. The charged Higgs signal samples are generated using PYTHIA [21], with the charged Higgs boson forced to decay purely into $\tau\bar{\nu}$ for the tauonic model or $c\bar{s}$ for the leptophobic model. The SM $t\bar{t}$ samples are generated with ALPGEN [22] for the matrix elements and parton showers followed by PYTHIA for the hadronization.

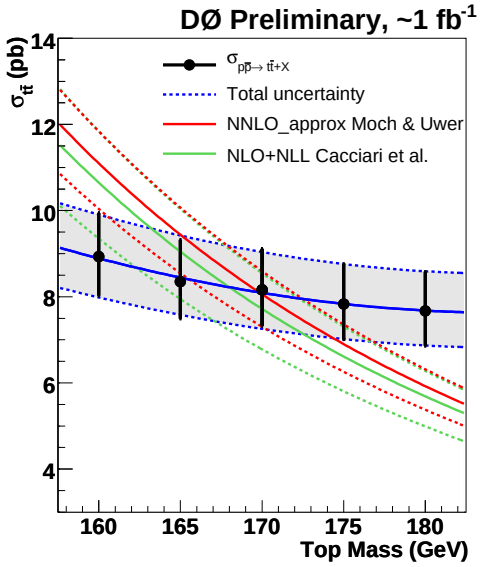

FIG. 3: Combined $t\bar{t}$ cross section as a function of top quark mass compared to the theoretical predictions from [23] and [17].

	$\sigma_{t\bar{t}}$	$+\sigma$	$-\sigma$
Statistical only	7.88	+0.47	-0.46
Source	Offset	$+\sigma$	$-\sigma$
Lepton identification	+0.02	+0.15	-0.14
Tau identification	+0.00	+0.02	-0.02
Jet identification	-0.03	+0.11	-0.11
Jet corrections	-0.09	+0.19	-0.16
Jet trigger in tau-sample	+0.00	+0.01	-0.00
Tau energy scale	+0.00	+0.02	-0.02
Trigger	-0.01	+0.11	-0.07
b-jet identification	+0.35	+0.34	-0.32
Signal modeling	+0.01	+0.17	-0.15
Background modeling	+0.01	+0.14	-0.14
Instrumental background	-0.02	+0.12	-0.12
Fake and real lepton rate estimate	-0.00	+0.03	-0.03
Other	-0.00	+0.15	-0.14
Total systematics	+0.24	+0.75	-0.66
	$\sigma_{t\bar{t}}$	$+\sigma$	$-\sigma$
Total error (excluding luminosity)	8.16	+0.80	-0.72

TABLE III: Combined $\sigma_{t\bar{t}}$ and its systematic uncertainties in the ℓ+jets, dilepton and τ+lepton channel. The "Offset" column shows either the central value of the fit (first and last lines) or the shift of the central value resulting from a particular source of systematics. The first line shows $\sigma_{t\bar{t}}$ with statistical uncertainty. The last line shows the result with all systematics included.

For a tauonic charged Higgs decay the number of expected $t\bar{t}$ events in the channels not containing τ decreases with increasing branching ratio $t \to H^+b$, while the number of expected events in the $\ell+\tau$ channel increases. In case of the leptophobic charged Higgs model, the number of expected events decreases in all considered channels with increasing $\mathcal{B}r(t \to H^+b)$ but at different rates.

We derive the event selection efficiencies for the three following scenarios:

- $t\bar{t} \to W^+b\,W^-\bar{b}$ (referred to as $t\bar{t} \to WW$)
- $t\bar{t} \to W^+b\,H^-\bar{b}$ (referred to as $t\bar{t} \to WH$)
- $t\bar{t} \to H^+b\,H^-\bar{b}$ (referred to as $t\bar{t} \to HH$)

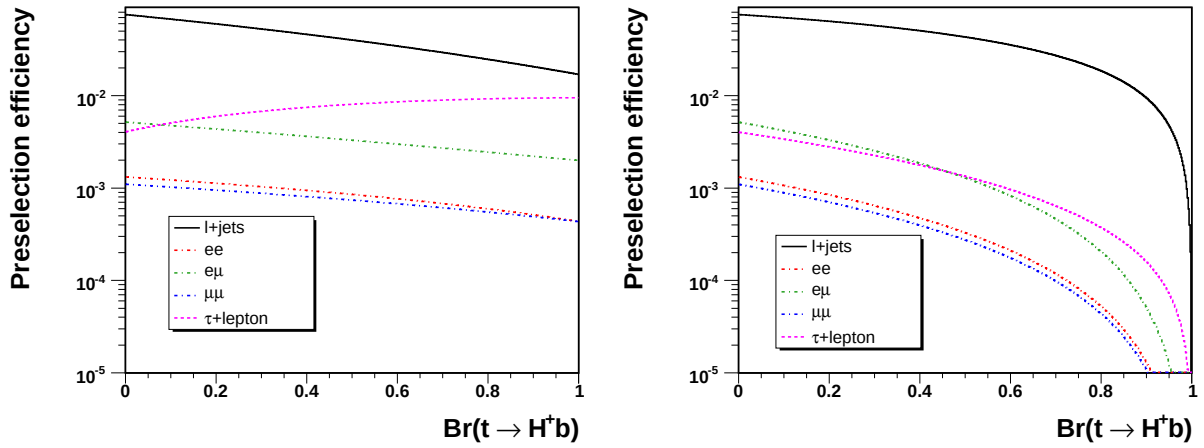

FIG. 4: Preselection efficiency as a function of $\mathcal{B}r(t \to H^+b)$ for a charged Higgs mass of 80 GeV for different search channels for tauonic (left) and leptophobic (right) models.

by selecting specific final states at the Monte Carlo truth level.

The total efficiency is a product of the preselection and b-tagging efficiencies:

$$\begin{aligned} P_{total}(t\bar{t}) &= (1-X)^2 P_p(t\bar{t} \to WW) P_b(t\bar{t} \to WW) + 2X(1-X) P_p(t\bar{t} \to WH) P_b(t\bar{t} \to WH) \\ &+ X^2 P_p(t\bar{t} \to HH) P_b(t\bar{t} \to HH), \end{aligned}$$

where P_p refers to the preselection efficiency. P_b is the probability to tag an event of a specified final state ($P_b = 1$ if no b-jet identification was applied) and $X = \mathcal{B}r(t \to H^+b)$.

In case of the tauonic and leptophobic charged Higgs models the acceptance $P_{total}(t\bar{t})$ depends mainly on the preselection efficiency P_p. When the charged Higgs boson mass approaches the top quark mass, the phase space for the b-quark becomes smaller, resulting in a decreasing probability P_b to tag an event with increasing $\mathcal{B}r(t \to H^+b)$.

Figure 4 shows the dependence of the preselection efficiency on $\mathcal{B}r(t \to H^+b)$ for all search channels and tauonic (left plot) and leptophobic model (right) for a charged Higgs mass of 80 GeV.

VI. LIMITS ON THE BRANCHING RATIO $\mathcal{B}r(t \to H^+b)$

In order to extract the branching ratio of a top quark decay to charged Higgs and a b-quark we calculate the predicted number of events in 14 search channels for various charged Higgs masses and branching ratios and perform a maximum likelihood fit to the number of observed events in data. The procedure is similar to the combination of the $t\bar{t}$ cross section measurements but now the $\mathcal{B}r(t \to H^+b)$ is implemented as a free parameter to be extracted from the fit. The $t\bar{t}$ cross section is set to 7.3 ± 0.7 pb corresponding to the theoretical next-to-leading order calculation at the current world average top quark mass of 172.6 GeV [16, 17]. The uncertainty on the theoretical cross section includes the uncertainty on the world average top quark mass of 1.4 GeV.

We extract upper limits on $\mathcal{B}r(t \to H^+b)$ for the two considered models. We set the limit following the likelihood ordering principle of Feldman and Cousins [24]. To determine the limits we generate ensembles for various input values $\mathcal{B}r_{\text{true}}$ taking into account all systematic uncertainties and their correlations. Feldman-Cousins confidence level bands for an 80 GeV charged Higgs decaying tauonically are shown in Fig.5.

Figures 6 and 7 show the expected and observed upper 95% C. L. limit on $\mathcal{B}r(t \to H^+b \to \tau^+\nu b)$ and $\mathcal{B}r(t \to H^+b \to c\bar{s}b)$ as a function of charged Higgs boson mass along with the one standard deviation band around the expected limit.

Table IV shows an example of the systematic uncertainties on $\mathcal{B}r(t \to H^+b)$ for a charged Higgs mass of 80 GeV in the tauonic charged Higgs model. The main sources of systematic uncertainty on $\mathcal{B}r(t \to H^+b)$ include the uncertainty on the luminosity of 6.1 % and the $t\bar{t}$ cross section. These two dominant systematic uncertainties are approximately of the same size as the statistical uncertainty on $\mathcal{B}r(t \to H^+b)$.

We compare the limits for the tauonic and leptophobic models with a tree level calculation of $\mathcal{B}r(t \to H^+b)$ in the MSSM using Eq. (12) of [25] with $m_t = 172.6$ GeV, $m_b = 4.8$ GeV, $m_W = 80.4$ GeV. The tauonic charged Higgs model (Fig.6) represents the MSSM in the region of $\tan\beta \geq 15$.

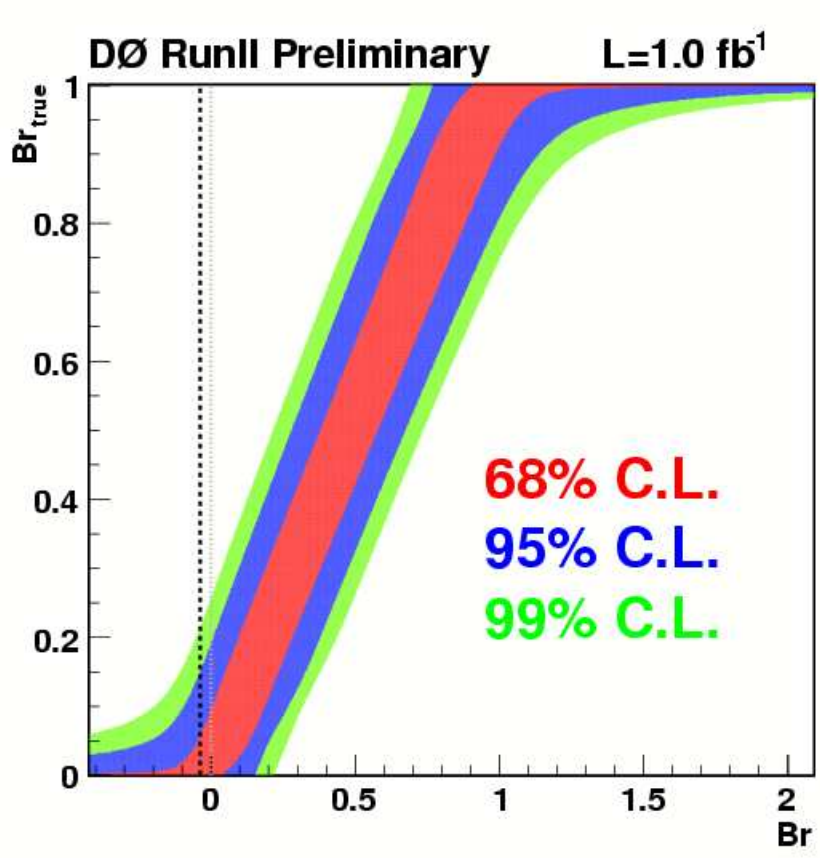

FIG. 5: Feldman-Cousins confidence level bands for $\mathcal{B}r(t \to H^+b)$ for tauonic decaying charged Higgs with mass of 80 GeV.

The leptophobic model with a branching ratio $\mathcal{B}r(H^+ \to c\bar{s}) = 100$ % can be similar to different SUSY models at small $\tan\beta$ (Fig.7). Examples are 2HDM models [4] or the MSSM [5, 6] with an additional suppression of $H^+ \to \tau^+\nu$ decays which could emerge from large radiative corrections from SUSY-breaking effects. [4–6]. Another example is the MHDM, where $\mathcal{B}r(H^+ \to c\bar{s}) = 100$ % is possible. In the MHDM, $\mathcal{B}r(t \to H^+b)$ depends not on $\tan\beta$ but instead on the respective coupling between the charged Higgs, the right-handed up-type quark field and the left-handed down-type quark field [4]. Therefore in case of the MHDM in Eq. (12) of [25] and in Figs. 7 and 11 $\tan\beta$ has to be replaced by the MHDM coupling.

Table V shows the lower 95% C. L. limits on the charged Higgs mass for large $\tan\beta$ for the tauonic model, and for small $\tan\beta$ for the leptophobic model.

VII. MODEL-INDEPENDENT MEASUREMENT OF $\sigma_{t\bar{t}}$ AND $\mathcal{B}r(t \to H^+b)$ IN THE TAUONIC CHARGED HIGGS MODEL

In the previous section the fit of the branching ratio $\mathcal{B}r(t \to H^+b)$ was performed with a fixed value for the $t\bar{t}$ cross section using the theoretical prediction at the world average top quark mass. Here we fit $\sigma_{t\bar{t}}$ and $\mathcal{B}r(t \to H^+b)$ simultaneously for the tauonic model. In the two dimensional fit the limit becomes independent of any assumption about the theoretical $t\bar{t}$ cross section and the corresponding large uncertainty does not affect the limit. In addition, another large uncertainty, the luminosity uncertainty, is fully absorbed by the fitted cross section.

The fitting procedure is the same as for the one dimensional fit of $\mathcal{B}r(t \to H^+b)$. We perform the fit of both quantities for each charged Higgs boson mass. The limit on the charged Higgs branching ratio is then obtained with the Feldman Cousins method. For the ensemble generation the cross section is set to the measured value. For the fit to the pseudo-data $\sigma_{t\bar{t}}$ and $\mathcal{B}r(t \to H^+b)$ are allowed to float, resulting in the full inclusion of the larger statistical and the different systematic uncertainties due to the 2D fit into the limit on $\mathcal{B}r(t \to H^+b)$. Figure 8 shows the 68% and 95% C.L. contours for the result of the fit for the charged Higgs masses of 80 GeV (left) and 120 GeV (right) with

Source	$+\sigma$	$-\sigma$
Statistical uncertainty	0.047	-0.046
Lepton identification	0.010	-0.010
Tau identification	0.007	-0.006
Jet identification	0.010	-0.010
Jet corrections	0.020	-0.019
Jet trigger in tau sample	0.002	-0.000
Tau energy scale	0.004	-0.004
Trigger	0.007	-0.006
b-jet identification	0.030	-0.030
Signal modeling	0.010	-0.010
Background modeling	0.010	-0.010
Instrumental background	0.019	-0.016
Fake and real lepton rate estimate	0.003	-0.003
$t\bar{t}$ cross section uncertainty	0.051	-0.052
Luminosity	0.032	-0.027
Other	0.010	-0.010
Total systematic	0.077	-0.075

TABLE IV: Statistical and systematic uncertainties for $\mathcal{B}r(t \to H^+b)$ for charged Higgs mass of 80 GeV and tauonic model. For this example the central value is found to be $\mathcal{B}r(t \to H^+b) = -0.053$.

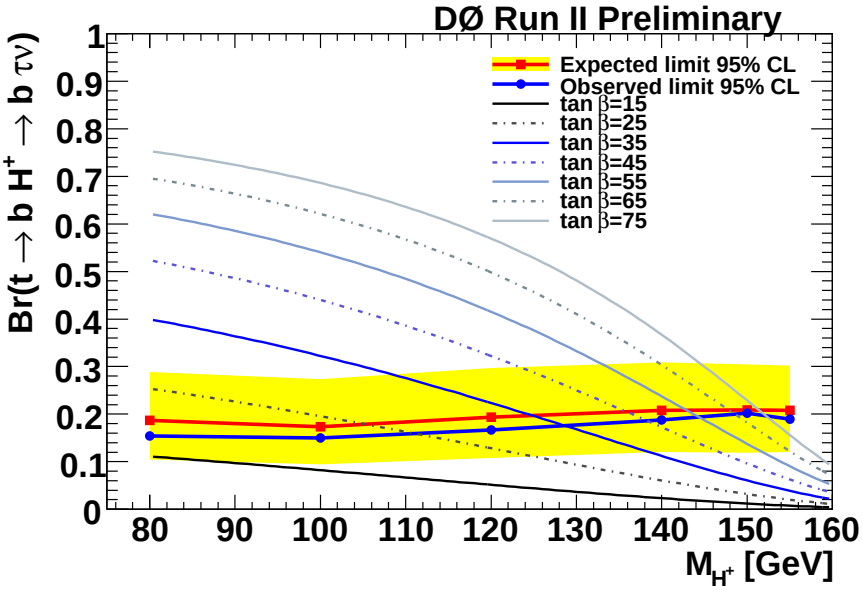

FIG. 6: Observed (blue) and expected (red) limit with one standard deviation band (yellow) in the MSSM on $\mathcal{B}r(t \to H^+b)$ versus charged Higgs mass.

statistical uncertainty only. The shape of the contours indicates an increased correlation between the two observables as the charged Higgs mass increases.

Figure 9 and Figure 10 show the fitted $t\bar{t}$ cross section and the resulting limits on the $\mathcal{B}r(t \to H^+b)$ for different charged Higgs masses. For small charged Higgs boson masses, a simultaneous fit provides about 30% improvement compared to the limits obtained with the one-dimensional fit.

Fig. 11 shows exclusion contours in the m_{H^+} versus $\tan\beta$ parameter space. Assuming the MSSM in the large $\tan\beta$ region dominated by the tauonic decaying charged Higgs and the leptophobic model in the small $\tan\beta$ region, we can exclude charged Higgs masses up to 150 GeV depending on $\tan\beta$.

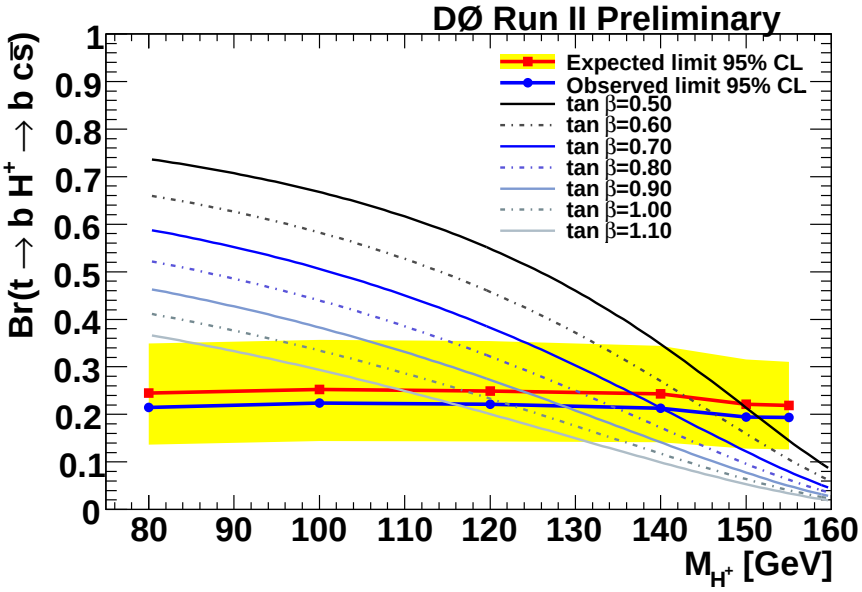

FIG. 7: Observed (blue) and expected (red) limit with one standard deviation band (yellow) in the leptophobic model on $\mathcal{B}r(t \to H^+b)$ versus H^+ mass.

$\tan\beta$	$H^\pm$ mass limit (GeV)
0.50	151
0.60	146
0.70	140
0.80	134
0.90	129
1.0	122
1.1	115
15	none
25	113
35	130
45	139
55	145
65	149
75	153

TABLE V: Lower mass 95% C. L. limits on the charged Higgs mass for the tauonic model at large $\tan\beta$ and leptophobic model at small $\tan\beta$. The calculations are at tree level.

VIII. SUMMARY

We combined the $t\bar{t}$ cross section of the ℓ+jets, dilepton and $\ell + \tau$ channels. The result is

$$\sigma_{\bar{t}} \;=\; 7.83^{+0.77}_{-0.70}(\text{stat+syst}) \pm 0.48(\text{lumi})\ \text{pb}\ .$$

for a top quark mass of 175 GeV. Furthermore, we performed a search for charged Higgs bosons in top quark decays, assuming a theoretical NLO SM $t\bar{t}$ cross section of 7.3 ± 0.7 pb. No indication for charged Higgs boson production in the tauonic or leptophobic model was found. For the tauonic model we exclude branching fractions from above 0.16 to above 0.2 for the charged Higgs mass range between 80 and 155 GeV. For the leptophobic charged Higgs decay we exclude branching fraction above 0.2 for the same mass range. For the tauonic decaying charged Higgs bosons we performed a model-independent measurement of $\mathcal{B}r(t \to H^+b)$ and excluded branching fractions from above 0.12 to above 0.26 depending on the charged Higgs mass.

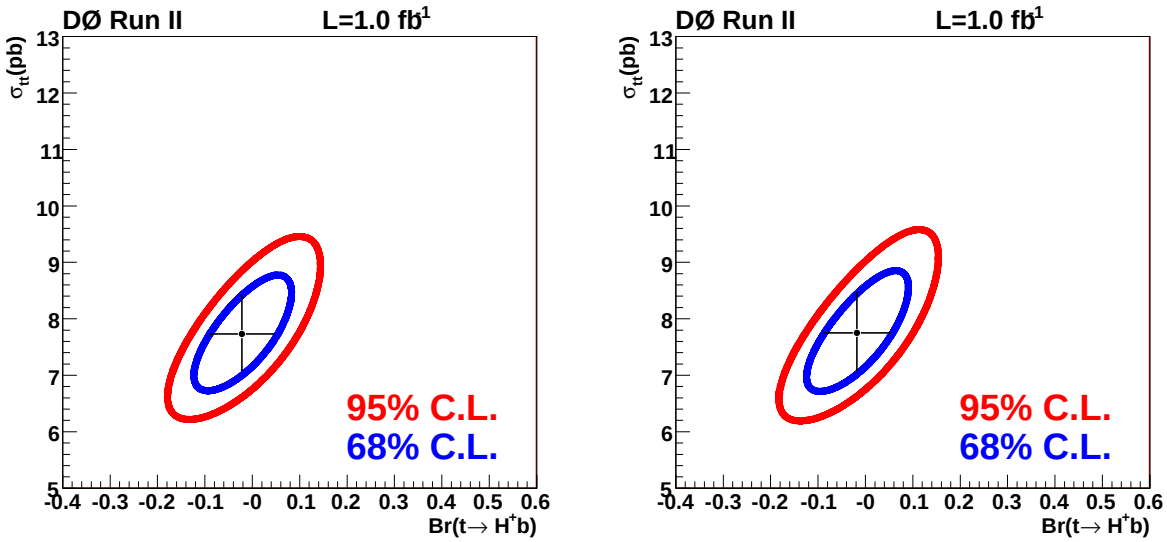

FIG. 8: Contour plot for a two-dimensional fit of $Br(t \to H^+b)$ and $\sigma_{t\bar{t}}$ for the charged Higgs mass of 80 GeV (left) and 120 GeV (right). Statistical uncertainty only is included.

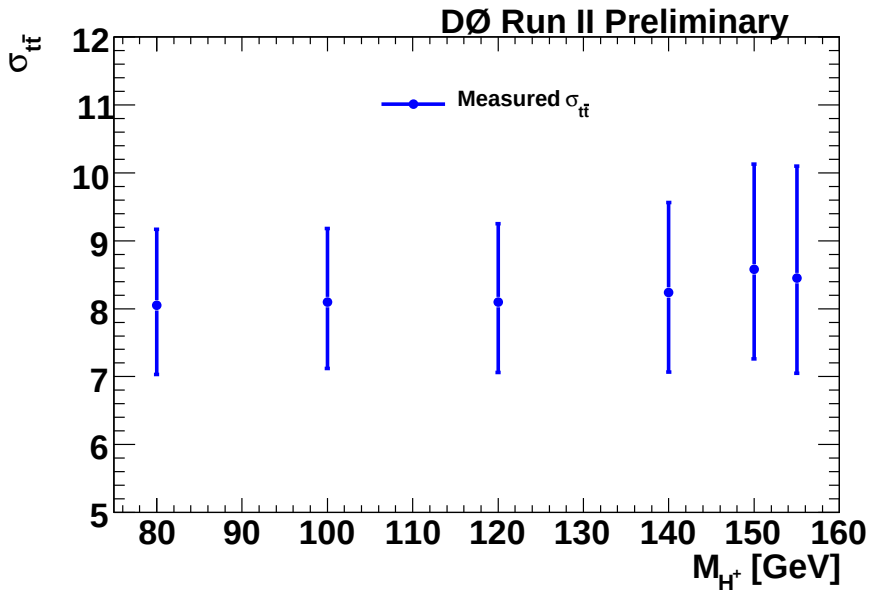

FIG. 9: Fitted $t\bar{t}$ cross section versus charged Higgs mass for tauonic charged Higgs model.

Acknowledgments

We thank the staffs at Fermilab and collaborating institutions, and acknowledge support from the Department of Energy and National Science Foundation (USA), Commissariat à l'Energie Atomique and CNRS/Institut National de Physique Nucléaire et de Physique des Particules (France), Ministry of Education and Science, Agency for Atomic Energy and RF President Grants Program (Russia), CAPES, CNPq, FAPERJ, FAPESP and FUNDUNESP (Brazil), Departments of Atomic Energy and Science and Technology (India), Colciencias (Colombia), CONACyT (Mexico), KRF (Korea), CONICET and UBACyT (Argentina), The Foundation for Fundamental Research on Matter (The Netherlands), PPARC (United Kingdom), Ministry of Education (Czech Republic), Natural Sciences and Engineering

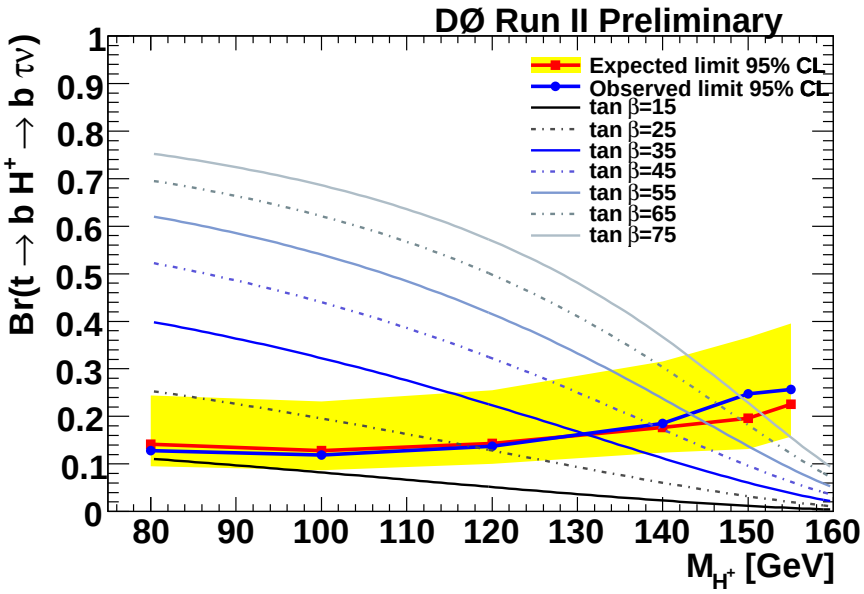

FIG. 10: Observed (blue) and expected (red) limit with one standard deviation band (yellow) on $\mathcal{B}r(t \to H^+b)$ as a function of charged Higgs mass for simultaneous fit of $\mathcal{B}r(t \to H^+b)$ and $\sigma_{t\bar{t}}$ in the tauonic model.

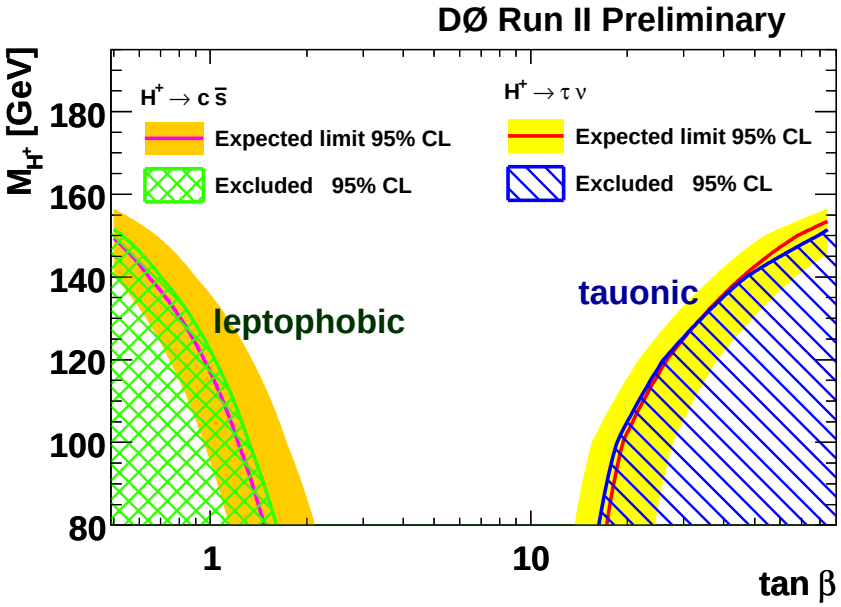

FIG. 11: Observed (blue) and expected (red) limit with one standard deviation band (yellow) on charged Higgs mass as a function of $\tan\beta$.

Research Council and WestGrid Project (Canada), BMBF (Germany), A.P. Sloan Foundation, Civilian Research and Development Foundation, Research Corporation, Texas Advanced Research Program, and the Alexander von Humboldt Foundation.

[1] Comput. Phys. Commun. **156**, 283 (2004).

[2] R. Eusebi, Ph.D. thesis, University of Rochester, FERMILAB-THESIS-2005-33 (2005).
[3] Y. Grossman, Nucl. Phys. B **426**, 355 (1994).
[4] A. G. Akeroyd, hep-ph/9509203 (1995).
[5] M. S. Carena, S. Mrenna and C. E. M. Wagner, Phys. Rev. D **62**, 055008 (2000).
[6] M. Spira, private communication.
[7] CDF Collaboration, A. Abulencia *et al.*, Phys. Rev. Lett. **96**, 042003 (2006).
[8] CDF Collaboration, A. Abulencia *et al.*, CDF note 9322 (2008).
[9] DØ Collaboration, V. Abazov *et al.*, Nucl. Instrum. and Methods A **565**, 463 (2006).
[10] Rapidity y and pseudorapidity η are defined as functions of the polar angle θ and parameter β as $y(\theta,\beta) \equiv \frac{1}{2}\ln\left[(1+\beta\cos\theta)/(1-\beta\cos\theta)\right]$ and $\eta(\theta) \equiv y(\theta,1)$, where β is the ratio of a particle's momentum to its energy.
[11] Impact parameter is defined as the distance of closest approach (d_{ca}) of the track to the primary vertex in the plane transverse to the beamline. Impact parameter significance is defined as $d_{ca}/\sigma_{d_{ca}}$, where $\sigma_{d_{ca}}$ is the uncertainty on d_{ca}.
[12] V. Abazov *et al.*, FERMILAB-PUB-05-034-E (2005).
[13] DØ Collaboration, V. Abazov *et al.*, Phys. Rev. Lett. **100**, 192003 (2008).
[14] DØ Collaboration, DØ note 5451-CONF (2007).
[15] DØ Collaboration, DØ note 5371-CONF (2007).
[16] N. Kidonakis and R. Vogt, Phys. Rev. D **68**, 114014 (2003) and private communication.
[17] M. Cacciari *et al.*, J. High Energy Phys. **404**, 68 (2004).
[18] The Tevatron Electroweak working group, arXiv.org:0803.1683 (2008).
[19] P. Sinervo, in *Proceedings of Statistical methods in Particle Physics, Astrophysics, and Cosmology*, edited by L. Lyons, R. P. Mount, and R. Reitmeyer (SLAC, Stanford, 2003), p. 334.
[20] T. Scanlon, Ph.D. thesis, University of London, 2006. FERMILAB-THESIS-2006-43.
[21] T. Sjöstrand, L. Lonnblad, S. Mrenna, PYTHIA 6.3: Physics and manual, hep-ph/0308153 (2003).
[22] M.L. Mangano *et al.*, JHEP **07**, 001 (2003).
[23] S. Moch and P. Uwer, arXiv:0804.1476 (2008).
[24] G. Feldman and R. Cousins, Phys. Rev. D **57**, 3873 (1998).
[25] J. A. Coarasa, D. Garcia, J. Guasch, R. A. Jimenez and J. Sola, Eur. Phys. J. C **2**, 373 (1998).